Journal of ELECTRONIC MATERIALS
DOI: 10.1007/s11664-010-1503-y

The Influence of Film Thickness on the Transparency and Conductivity of Al-Doped ZnO Thin Films Fabricated by Ion-Beam Sputtering

GUANG-XING LIANG,[1] PING FAN,[1,2] XING-MIN CAI,[1] DONG-PING ZHANG,[1] and ZHUANG-HAO ZHENG[1]

1.—Institute of Thin Film Physics and Application, College of Physics Science and Technology, Shenzhen University, Shenzhen 518060, China. 2.—e-mail: fanping@szu.edu.cn

To evaluate the influence of film thickness on the structural, electrical, and optical properties of Al-doped ZnO (AZO) films, a set of polycrystalline AZO samples with different thickness were deposited on glass substrates by ion-beam sputtering deposition (IBSD). X-ray diffraction (XRD), atomic force microscopy (AFM), energy-dispersive x-ray spectroscopy (EDS), four-point probe measurements, and spectrophotometry were used to characterize the films. XRD showed that all the AZO films had preferred *c*-axis orientation. The ZnO (110) peak appeared, and the intensity increased, with increasing thickness. All the samples exhibited compressive intrinsic stresses. AFM showed that the grain size along with the root-mean-square (RMS) roughness increased with increasing thickness. The decrease of resistivity is due to the corresponding change in grain size, surface morphology, and chemical composition. The average optical transmittance of the AZO films was over 80%, and a sharp fundamental absorption edge with red-shifting was observed in the visible region. The optical band gap decreased from 3.95 eV to 3.80 eV when the AZO film thickness increased from 100 nm to 500 nm.

Key words: Al-doped ZnO, ion-beam sputtering, microstructure, electrical and optical properties

INTRODUCTION

Zinc oxide (ZnO)-based material is one of the most interesting transparent conducting oxides (TCOs). It is a potential substitute for indium tin oxide (ITO) in all corresponding applications, such as plasma displays, liquid-crystal displays, transparent conducting films for solar cells, and other optoelectronic devices. Pure or Al-doped ZnO (AZO) films have been considered as possible transparent conducting materials since they present high conductivity, good optical transmittance, and low-cost fabrication.[1–5] For the preparation of AZO films, various techniques have been employed, such as magnetron sputtering,[6–8] thermal evaporation,[9] pulsed laser deposition (PLD),[10] chemical vapor deposition (CVD),[11] molecular-beam epitaxy (MBE),[12] sol gel,[13] and spray pyrolysis.[14] However, little attention has been devoted to AZO films prepared by ion-beam sputtering deposition (IBSD). Compared with those techniques, IBSD has several advantages such as excellent stoichiometry transfer of the target material, good uniformity, and simple setup required for film formation. In addition, IBSD can be realized at lower vacuum pressure. Thus, optimization of AZO film properties by IBSD could be expected. Seong et al.[15] reported the influence of substrate temperature on AZO properties. Film thickness also has considerable effects on its structural, electrical, and optical properties. Tanaka et al.[16] reported the electrical properties and atomic force microscopy (AFM) analysis of AZO films prepared by PLD from 200 nm to 1000 nm thick. Tadatsugu et al.[17] reported that the resistivity of AZO films was very unstable below about 50 nm. Dong et al.[10] reported

(Received March 25, 2010; accepted December 20, 2010)

Published online: 29 January 2011

the effect of thickness on the properties of AZO films, and the results demonstrated that the structural, optical, and electrical properties could be optimized with a thickness above 120 nm. In this work, the effects of thickness (from 100 nm to 500 nm) on the structural, surface morphology, electrical, and optical properties of AZO films prepared by IBSD were investigated.

EXPERIMENTAL PROCEDURES

AZO thin films were prepared on BK7 glass substrates by ion-beam sputtering. A 110 mm × 110 mm × 3 mm square-shaped ceramic target of ZnO (99.9% purity) mixed with 2 wt.% Al_2O_3 (99.9% purity) was employed. Before sputtering, the vacuum chamber was evacuated to base pressure of 4.0×10^{-4} Pa. High-purity (99.99%) Ar (6 sccm) was introduced, and deposition was carried out at working pressure of 3.0×10^{-2} Pa after presputtering for about 20 min to remove contaminants from the surface of the target. The substrate temperature was fixed to be about 200°C; more details on sample preparation are given in Table I.

The thickness of the AZO films was measured using a DEKTAK 150 profilometer. The microstructure of AZO films was investigated by x-ray diffraction (XRD) (ax5-D8-ADVANCE, BRUKER) using Cu K_α radiation (λ = 0.15406 nm). The chemical composition of the AZO films was determined by using an energy-dispersive x-ray microanalysis system (EDS). The surface morphology and root-mean-square (RMS) surface roughness were characterized using an atomic force microscopy (AFM, CSPM5500) in contact mode. The electrical sheet resistance R_s was determined using the four-point probe method, and the resistivity ρ was obtained using $\rho = R_s d$, where d is the film thickness. Optical transmittance was obtained by ultraviolet (UV)/visible/near-infrared (NIR) spectrophotometry (Lambda 900, PerkinElmer).

RESULTS AND DISCUSSION

Structure and Surface Morphology

Figure 1 shows x-ray diffraction (XRD) patterns of the AZO films deposited on BK7 glass substrates. The film thickness is from 100 nm to 500 nm. The

Table I. The ion-beam sputtering parameters used for preparing AZO thin films

	Voltage (V)	Current (A)	Plasma Energy (keV)
Screen	–	–	1.3
Anode	80	0.2	–
Acceleration	250	0.01	–
Cathode	10	12	–
Beam	–	0.02	–
Neutral	–	3.5	–

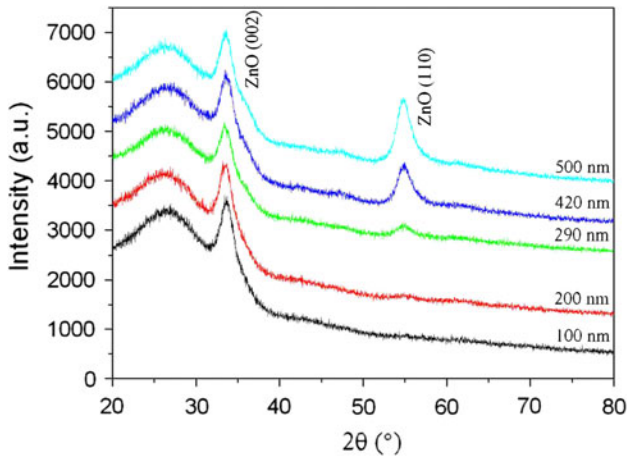

Fig. 1. XRD patterns of AZO thin films with different thickness.

broad peak around 26° is due to the amorphous nature of the glass substrate. All the AZO films with different thickness showed a strong (002) peak at 2θ near 34°. No peaks related to metallic Zn or Al_2O_3 were observed. The diffraction patterns show that the deposited AZO films exhibit a hexagonal structure, which indicates that the replacement of Zn^{2+} (ionic radius ~0.74 Å) with Al^{3+} ions (~0.51 Å) does not change the hexagonal wurtzite structure. In fact, ZnO (002) peaks are the preferred orientation when the thickness is 100 nm and 200 nm with no trace of ZnO (110) peak. The ZnO (110) peak appears, and the intensity increases, with increasing thickness. This experimental result is similar to our latest report.[18]

Figure 2 shows the variations of ZnO (002) diffraction angle with increasing thickness. The ZnO (002) peaks are located at 2θ = 33.67°, 33.52°, 33.38°, 33.42°, and 33.48°, respectively. The (002) diffraction peak shifts towards lower angles as compared with standard data (2θ = 34.43°), which implies that the c-axis lattice constant is expanded. This also suggests the existence of residual stress in the AZO films. This stress may result from the linear expansion coefficient difference between the AZO thin film and the glass substrate, or come from defects, such as O vacancies (V_O), Zn interstitials (i_{Zn}), Al interstitials (i_{Al}), etc. It is reported that the strain induced by the linear expansion coefficient mismatch between the film and the glass substrate is not the major origin of the (002) diffraction angle variations.[19] The strain in the c-axis could be expressed by the formula

$$\varepsilon = \frac{d - d_0}{d_0}, \quad (1)$$

where d and d_0 are the strained and unstrained lattice coefficient, respectively. The lattice coefficient could be calculated according to the Bragg formula and the peak positions in the XRD patterns. The calculated d-spacing for all the samples is

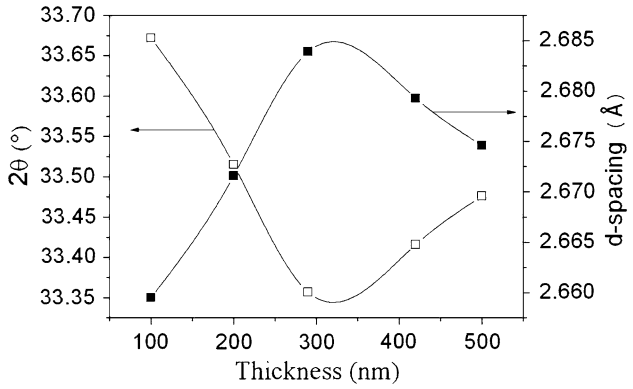

Fig. 2. The diffraction angle of the ZnO (002) peak and the *d*-spacing of the ZnO (002) plane as a function of film thickness.

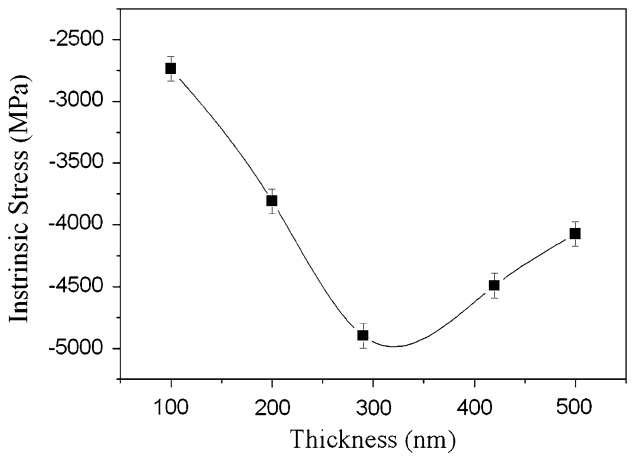

Fig. 3. Calculated stress in the ZnO as a function of film thickness.

shown in Fig. 2. The undoped ZnO thin films were prepared using the ion-beam sputtering method, and the corresponding unstressed lattice parameter d_0 (2.6286 Å) is found to be higher than that (2.6035 Å)[20] of bulk ZnO materials of similar composition, which is similar to the result of Wang et al.[21] The residual stress calculation is based on the biaxial strain model, and the following formula is used:[22]

$$\sigma = \frac{2c_{13}^2 - c_{33}(c_{11}+c_{12})}{2c_{13}} \cdot \frac{d-d_0}{d_0}; \qquad (2)$$

for the elastic constants c_{ij} of single-crystal ZnO, the following values were used: c_{11} = 208.8 GPa, c_{33} = 213.8 GPa, c_{12} = 119.7 GPa, and c_{13} = 104.2 GPa.[23] The calculated intrinsic stress for different thicknesses is shown in Fig. 3. The negative sign indicates that the stress of all AZO films is compressive. The compressive stress is about 2737 MPa at thickness of 100 nm, and 3809 MPa at 200 nm. The stress increases to about 4898 MPa at 290 nm and then decreases to 4074 MPa at 500 nm. The evolution of stress as a function of thickness is similar to the data in the literature.[23] Smaller Al^{3+} substituting for Zn^{2+} is believed to shrink the ZnO lattice and reduce the magnitude of the stress. However, there is more interstitial Al^{3+} in ZnO. This results in the lattice constant expansion and the generation of stress. Increasing the thickness, within a suitable range, increases the transfer ability of surface atoms, which leads to accelerated crystallization of AZO films via small grain aggregation. Consequently, reduction of structural defects was achieved, and relaxation of the AZO films is observed.

AFM images of all the samples are shown in Fig. 4. The images indicate that the grain size increases with increasing thickness. In the AFM image of AZO film with 100 nm thickness, some small grains are found occasionally. Dong et al.[10] reported that the crystal grains become distinct with thickness changing from 56 nm to 120 nm and that the morphology of 580-nm-thick films changed from hillocky to cratered. In the AFM images of 420-nm- and 500-nm-thick films, larger grains are found, but some voids also appear. This suggests that the diffusion and transfer ability of surface atoms are improved with increasing thickness, which leads to accelerated crystallization of AZO films and hence the enhancement of surface roughness. The root-mean-square (RMS) roughness obtained from AFM measurement is shown in Fig. 5. In addition, the RMS roughness of the substrate is 0.16 nm. As seen in Fig. 5, AZO films of 100 nm thickness show a smooth surface with RMS of 1.41 nm. The RMS roughness gradually increases from 1.41 nm to 3.42 nm as the film thickness increases from 100 nm to 500 nm. The increase of roughness with increasing thickness mainly results from the corresponding change in grain size.

Film Composition

The chemical composition of the AZO films was analyzed by EDS spectroscopy. The detection limit of quantitative analysis is ~0.5 at.% for EDS, which is applicable to our cases. The atomic percentage (C_A) of the element in the matrix is given by[24]

$$C_A = \frac{(S_A I_A)}{\sum_i S_i I_i}, \qquad (3)$$

where S_A and I_A are the EDS sensitivity factor and the integral count of element A, respectively. For AZO film, i = 3 is the number of elements present, including Zn, O, and Al. Figure 6 shows the composition of AZO films with different thickness. The amount of Al is about 7.8 at.%, while the amount of Zn is 30.9 at.% and the amount of O is 61.3 at.% at thickness of 100 nm. With increasing thickness, the Al content is up to 11.7 at.% and the amount of O decreases to 37.0 at.%.

Electrical Properties

Figure 7 shows the resistivity as a function of film thickness for the AZO films. The electrical resistivity

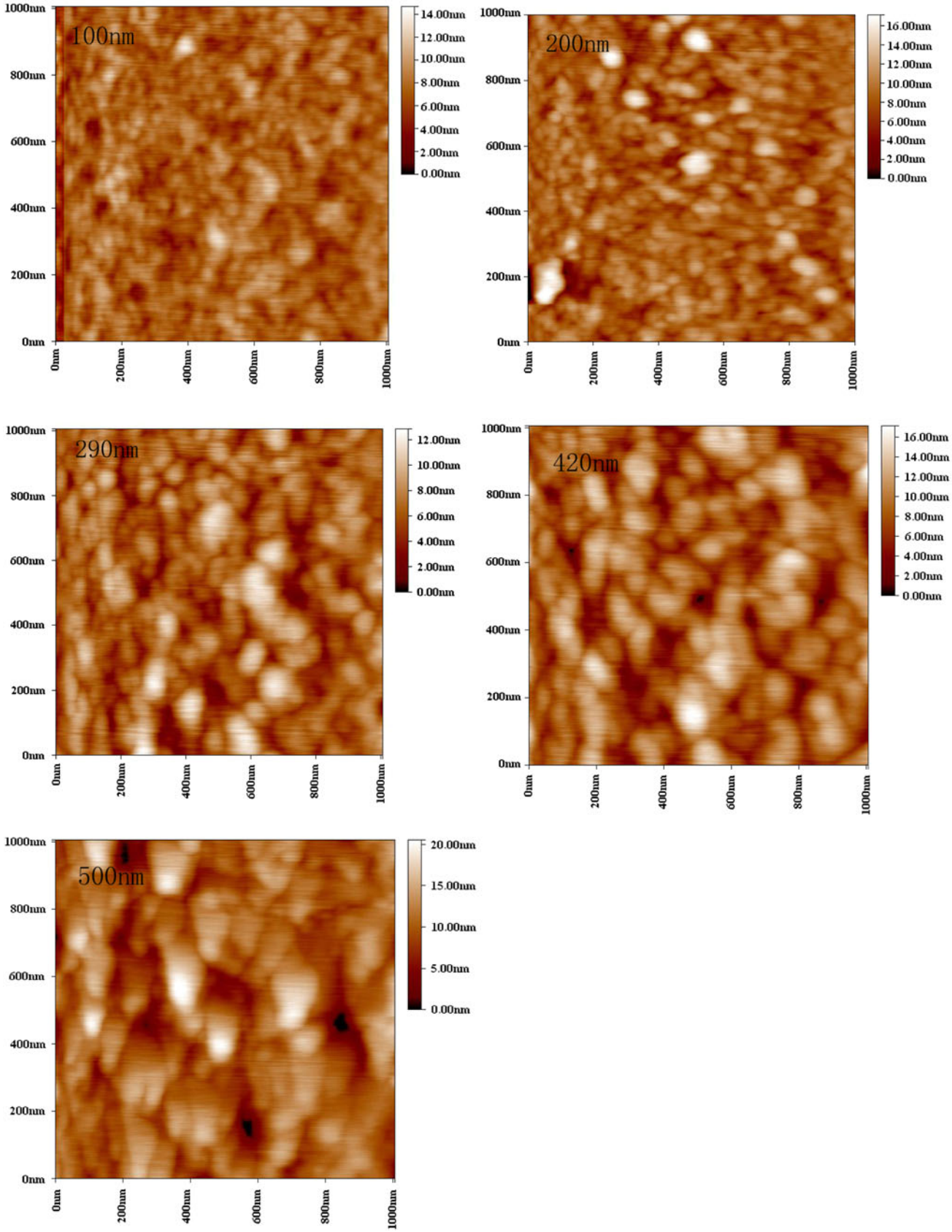

Fig. 4. AFM images (contact mode) of the AZO films with different thickness.

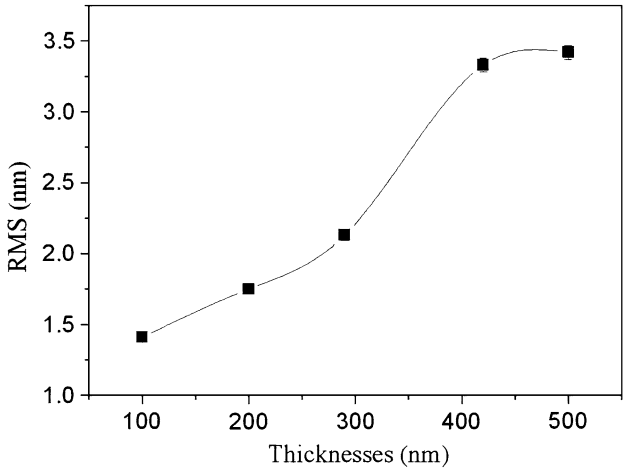

Fig. 5. RMS roughness of the AZO films as a function of film thickness.

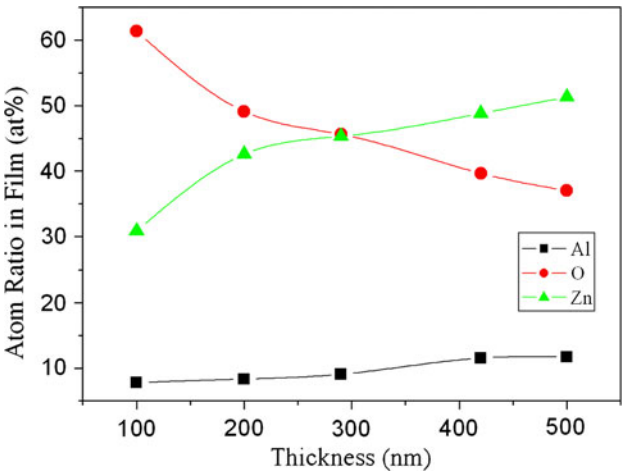

Fig. 6. Chemical composition of AZO films with different thickness.

decreases significantly with increasing thickness. As the thickness increases to 420 nm, the resistivity reaches a minimum value and then slightly increases over 420 nm. From these results, it can be seen that the film resistivity depends on the film thickness. This might be associated with different grain size, morphology, and chemical composition of AZO thin films. Improved crystallinity can be achieved with increasing thickness, as shown in Fig. 4. The AZO films of 420 nm and 500 nm thickness contained larger grains, but some voids appeared in 500-nm-thick AZO, which may be induced by continuous atom bombardment with high sputtering energy. Thus, the 420-nm-thick AZO films with the minimum resistivity value are reasonable, similar to reported results.[25,26] Generally, grain boundaries have a large effect on the electrical properties. Indeed, increase of grain size and improvement of crystallinity will lead to

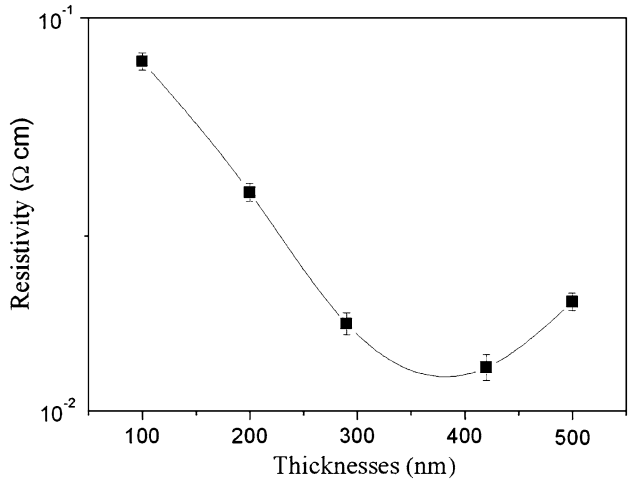

Fig. 7. Electrical resistivity of AZO films with different thickness.

decrease of grain boundaries and defects in the films, thus resulting in lower resistivity.

Optical Properties

Figure 8a shows the transmission spectra of the AZO thin films. The loss due to the glass substrate was removed during the measurement. The average transmittance of samples over visible wavelengths decreases from 85% to 80% with increasing thickness. The position and shape of the absorption edge depend on the film thickness. All the films exhibit a sharp absorption edge due to the direct transition of electrons from the valence band to the conduction band. A fall-off for wavelengths shorter than 332 nm is observed. Reported values for the sharp absorption edge are about 330 nm,[3,27] 50 nm,[20] and 380 nm.[24] Compared with these, the band gap of ZnO thin films is broadened in our work. In Fig. 8b, it can be found that the absorption edge shifts to longer wavelength (red-shifts) as the thickness increases from 100 nm to 500 nm. In a direct-band-gap semiconductor, the optical absorption coefficient (α) and the optical energy band gap (E_g) are related to each other by[28]

$$\alpha(h\upsilon) = C(h\upsilon - E_g)^{1/2}, \tag{4}$$

where C is a constant for direct transition, and $h\upsilon$ is the photon energy. From this relation, the optical energy band gap (E_g) is obtained by extrapolating the linear part of the spectrum $(\alpha h\upsilon)^2 = f(h\upsilon)$ to zero. As shown in Fig. 8c, the optical band gaps of AZO films decrease from 3.95 eV to 3.80 eV, which indicates a red-shift with increasing thickness. It is larger than those reported by Dong et al. (3.86 eV to 3.94 eV),[10] Yang et al. (3.75 eV to 3.86 eV),[29] and Ma et al. (3.78 eV).[30] The band gap energy of AZO films deposited with any thickness is larger than that of bulk ZnO (3.37 eV). Compared with intrinsic ZnO films, the contribution of substitutional Al^{3+} ions and interstitial Al atoms determines the band

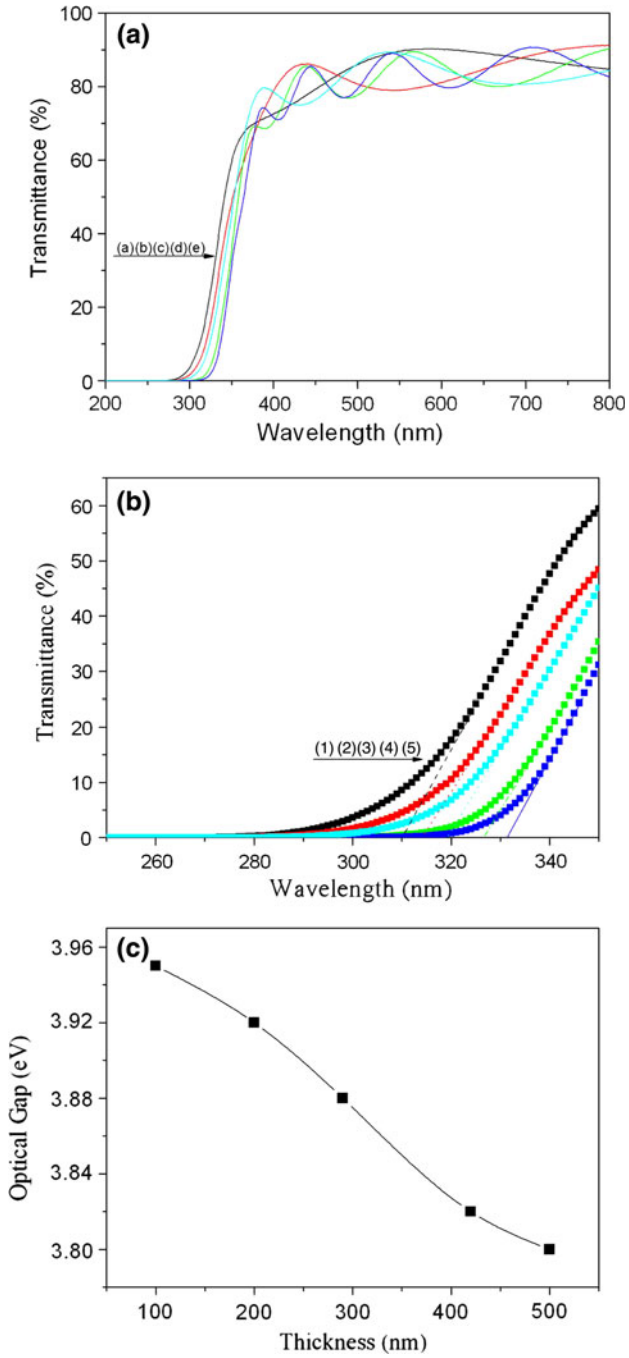

Fig. 8. (a) Transmittance spectra of AZO films with different thickness. (b) The optical band gaps as a function of thickness: (1) 100 nm, (2) 200 nm, (3) 290 nm, (4) 420 nm, and (5) 500 nm. (c) The variation of fundamental absorption edge with different thickness.

gap widening caused by the increase of carrier concentration, which can be explained by the Burstein–Moss shift.[31]

CONCLUSIONS

AZO films were deposited by IBSD on BK7 glass substrates. The influence of thickness on the properties of AZO films was investigated. All films showed a preferred *c*-axis orientation, but the (002) peak of the AZO films shifted to lower angles, compared with ZnO films. The ZnO (110) peak appeared, and the intensity increased, with increasing thickness, indicating that the crystalline quality of the films was improved. All the samples exhibited compressive stress. AFM images showed that the grain size and surface RMS roughness are obviously influenced by the AZO film thickness. The grain size along with the RMS roughness increased with increasing thickness. Accordingly, it is found that AZO films with thickness of 420 nm have the lowest electrical resistivity, which might be attributed to the change in grain size, surface morphology, composition, etc. The optical transmittance of AZO films was over 80% in the visible region, and red-shift of the optical absorption edge was observed. The optical band gap decreased from 3.95 eV to 3.80 eV with increasing thickness from 100 nm to 500 nm. In conclusion, IBSD can also be a suitable technique for fabricating high-quality AZO thin films.

ACKNOWLEDGEMENTS

The work was supported by the Natural Science Foundation of Guangdong Province in China (No. 7009409) and the Program of Science and Technology of Shenzhen, China (No. 200729).

REFERENCES

1. F.K. Shan, G.X. Liu, W.J. Lee, G.H. Lee, I.S. Kim, and B.C. Shin, *J. Cryst. Growth* 284, 277 (2007).
2. S.J. Henley, M.N.R. Ashfold, and D. Cherns, *Surf. Coat. Technol.* 271, 177 (2004).
3. B.Y. Oh, M.C. Geong, T.H. Moon, W. Lee, J.M. Myoung, J.Y. Hwang, and D.S. Seo, *J. Appl. Phys.* 99, 124505 (2006).
4. M. Hiramatsu, K. Imaeda, N. Horio, and M. Nawata, *J. Vac. Sci. Technol.* 16, 669 (1998).
5. D.C. Look and B. Claflim, *Phys. Status Solid B* 241, 624 (2004).
6. S.N. Bai and T.Y. Tseng, *J. Mater. Sci. Mater. Electron.* 20, 253 (2009).
7. S. Fernandez, A. Martinez-Steele, J.J. Gandia, and F.B. Na-ranjo, *Thin Solid Films* 517, 3152 (2009).
8. D.M. Zhu, K. Li, F. Luo, and W.C. Zhou, *Appl. Surf. Sci.* 255, 6145 (2009).
9. S.J. Jung, B.M. Koo, Y.H. Han, J.J. Lee, and J.H. Joo, *Surf. Coat. Technol.* 200, 862 (2005).
10. B.Z. Dong, G.J. Fangm, J.F. Wang, W.J. Guan, and X.Z. Zhao, *J. Appl. Phys.* 101, 033713 (2007).
11. M. Purica, E. Budianu, E. Rusu, M. Danila, and R. Gavrila, *Thin Solid Films* 485, 403 (2002).
12. T. Makino, K. Tamura, C.H. Chia, Y. Segawa, M. Kawasaki, and A. Ohtomo, *Phys. Status Solid B* 229, 853 (2002).
13. K.E. Lee, M.S. Wang, E.J. Kim, and S.H. Hahn, *Curr. Appl. Phys.* 9, 683 (2009).
14. P. Nunes, E. Fortunato, P. Tonello, F. Braz Fernandes, P. Vilarinho, and R. Martins, *Vacuum* 64, 281 (2002).
15. J.W. Seong, K.H. Kim, Y.W. Beag, S.K. Koh, and K.H. Yoon, *J. Vac. Sci. Technol. A* 22, 1139 (2004).
16. H. Tanaka, K. Ihara, T. Miyata, H. Sato, and T. Minami, *J. Vac. Sci. Technol. A* 22, 1757 (2004).
17. M. Tadatsugu, M. Toshihiro, O. Yuusuke, and K. Takeshi, *Phys. Stat. Sol. (RRL)* 1, 31 (2007).
18. D.P. Zhang, P. Fan, X.M. Cai, J.J. Huang, L.L. Ru, Z.H. Zheng, G.X. Liang, and Y.K. Huang, *Appl. Phys. A* 97, 434 (2009).

19. B.Z. Dong, H. Hu, G.J. Fang, X.Z. Zhao, D.Y. Zheng, and Y.P. Sun, *J. Appl. Phys.* 103, 073711 (2008).
20. X.Y. Li, H.J. Li, Z.J. Wang, H. Xia, Z.Y. Xiong, J.X. Wang, and B.C. Yang, *Opt. Commun.* 282, 247 (2009).
21. R.V. Wang, P. Mclntyre, J. Baniecki, K. Nomura, T. Shioga, K. Kurihara, and M. Ishii, *Appl. Phys. Lett.* 87, 192906 (2005).
22. R.J. Hong, H.J. Qi, J.B. Huang, H.B. He, Z.X. Fan, and J.D. Shao, *Thin Solid Films* 473, 58 (2005).
23. R. Cebulla, R. Wendt, and K. Ellmer, *J. Appl. Phys.* 83, 1087 (1998).
24. J.G. Lu, Z.Z. Ye, Y.J. Zeng, L.P. Zhu, L. Wang, J. Yuan, B.H. Zhao, and Q.L. Liang, *J. Appl. Phys.* 100, 073714 (2006).
25. I. Volintiru, M. Creatore, B.J. Kniknie, C.I.M.A. Spee, and M.C.M. van de Sanden, *J. Appl. Phys.* 102, 043709 (2007).
26. M. Suchea, S. Christoulakis, M. Katharakis, N. Vidakis, and E. Koudoumas, *Thin Solid Films* 517, 4303 (2009).
27. Th. Agne, Z. Guan, X.M. Li, H. Wolf, Th. Wichert, H. Natter, and R. Hempelmann, *Appl. Phys. Lett.* 83, 1204 (2003).
28. J.I. Pankove, *Optical Processes in Semiconductors* (New York: Dover, 1971), p. 143.
29. W.F. Yang, Z.G. Liu, D.L. Peng, F. Zhang, H.L. Huang, Y.N. Xie, and Z.Y. Wu, *Appl. Surf. Sci.* 255, 5669 (2009).
30. Q.B. Ma, Z.Z. Ye, H.P. He, L.P. Zhu, J.R. Wang, and B.H. Zhao, *Mater. Lett.* 61, 2460 (2007).
31. T.S. Moss, *Phys. Soc. Lond. B* 67, 775 (1954).